



Title	QoS-Oriented Mode, Spectrum, and Power Allocation for D2D Communication Underlying LTE-A Network
Author(s)	Asheralieva, Alia; Miyanaga, Yoshikazu
Citation	IEEE transactions on vehicular technology, 65(12), 9787-9800 https://doi.org/10.1109/TVT.2016.2531290
Issue Date	2016-12
Doc URL	http://hdl.handle.net/2115/64518
Rights	© 2016 IEEE. Personal use of this material is permitted. Permission from IEEE must be obtained for all other uses, in any current or future media, including reprinting/republishing this material for advertising or promotional purposes, creating new collective works, for resale or redistribution to servers or lists, or reuse of any copyrighted component of this work in other works.
Type	article (author version)
File Information	TVT-2015-00478-Final.pdf



[Instructions for use](#)

QoS Oriented Mode, Spectrum and Power Allocation for D2D Communication Underlying LTE-A Network

Alia Asheralieva and Yoshikazu Miyanaga, *Senior Member, IEEE*

Abstract — This paper investigates the problem of resource allocation for Device-to-Device (D2D) Communication in a Third Generation Partnership Project (3GPP) Long Term Evolution Advanced (LTE-A) network. The users in the network can operate either in a traditional cellular mode communicating with each other via the eNB, or in D2D mode communicating with each other without traversing the eNB. In the considered model, the D2D users and cellular users share the same radio resources. Particularly, each resource block (RB) within the available bandwidth can be occupied by one cellular and several D2D users. Hence, the problem of interference management is crucial for effective performance of such a network. The two-fold aim of the proposed algorithm is to i) mitigate the interference between cellular and D2D users and ii) improve the overall user-perceived quality of service (QoS). To control the interference, for each user we define a certain target interference level, and constrain the interference from the other users to stay below this level. The corresponding optimization problem maximizes the QoS of the users by minimizing the size of the buffers of user equipments (UEs). Performance of the algorithm has been evaluated using the OPNET-based simulations. The algorithm shows improved performance in terms of mean packet end-to-end delay and loss for UEs when compared to other relevant schemes.

Index Terms — Device-to-Device Communication, Interference Management, LTE-A, Resource Allocation.

I. INTRODUCTION

D2D communication has been proposed to increase spectral efficiency of cellular networks by allowing direct communication between two mobile users (called D2D users) without traversing the Base Station (BS) or core network [1]. D2D communication is also considered to be a new technological component for a 3GPP LTE-A system, aiming to reduce energy consumption, improve network utilization, and decrease end-to-end latency of cellular users [2]. In an underlay D2D model, the D2D users can reuse the licensed cellular spectrum and communicate directly with each other (while remaining controlled by the BS). Note that both the cellular and D2D users share the same radio resources, and therefore it is essential to control the interference caused by cellular users to D2D users, and vice versa [1]. Therefore, the problem of interference management is crucial for effective performance of such a network.

Many effective solutions have been proposed to combat this challenging problem and improve the overall performance of D2D-enabled cellular networks (see, e.g., [3] – [12]). Some of

these solutions (e.g., [3] – [5]) aim to increase the cellular spectrum efficiency by exploiting spatial diversity. Spectrum efficiency improvement is achieved either by reducing the interference (as in [3]) or by avoiding the interference ([4], [5]) among cellular and D2D users. The algorithm proposed in [3] uses a graph-based approach which accounts for the interference and capacity of a cellular network with underlay D2D communication. In the graph, each link (D2D or cellular) is represented by a graph vertex. The potential interference between the two links is represented by the edge connecting two vertices. Simulation results show that a graph-based approach performs close to the throughput-optimal resource allocation. In [4], instead of controlling, the interference is avoided by defining the so-called interference limited areas. These areas are formed according to the amount of tolerable interference and minimum signal-to-interference and noise (SINR) requirements for successful transmission. Different users (cellular or D2D) from the same interference area use different resources. Simulation results show a significant performance improvement achieved by this scheme (compared to the algorithms proposed previously). In [5], an iterative combinatorial auction game is proposed to allocate the spectrum resources and avoid intra-cell interference. In this game, the spectrum resources are regarded as the bidders, whereas the D2D links represent the goods. Based on the formulated game, the authors propose a non-monotonic descending price auction algorithm that converges in a finite number of iterations and shows improvement in sum-rate.

The methods presented in [6] – [8] focus on maintaining the certain QoS and/or power constraints of the users. Resource allocation method in [6] guarantees the QoS requirements of cellular/D2D users, formulated in terms of the total network throughput. Here a resource allocation problem is divided into three separate subproblems: (i) admission control, (ii) power control, (iii) maximum-weight bipartite matching. The authors benchmark performance of a proposed algorithm against performance of the previously proposed techniques, and show that the proposed resource allocation approach provides up to 70% throughput gain. In [7], a resource allocation problem is formulated as the system throughput maximization with minimum data rate constraints. A solution is obtained using the particle swarm optimization [12]. Simulation results show 15% throughput gain over the orthogonal resource sharing scheme, where the achievable gain varies with the distance of

D2D users. In [8], the problem of maximizing the mean sum-rate of a system is formulated as a stochastic optimization problem. A solution of the problem is found using the stochastic subgradient method. This solution is used to design a sub-channel opportunistic scheduling algorithm that takes into account the channel state information (CSI) of D2D/cellular links, as well as the QoS requirements of each D2D user. The numerical results show that the mean sum-rate can be improved by up to 500%, and this gain increases when the average distance between a pair of D2D users reduces.

The algorithms [9] – [11] are designated to enhance the power efficiency, spectrum utility and fairness. The algorithm proposed in [9] aims to minimize the total transmission power of the users, subject to link data rate, interference, channel allocation and power assignment constraints. Because of the complexity of a formulated problem, it is divided into three subproblems: mode selection, channel allocation and power assignment. To improve the efficiency of resource allocation, the authors present a polynomial-time heuristic algorithm that jointly solves these subproblems, and show that a proposed technique can achieve over 57% power savings, compared to several baseline methods. In [10], the user spectrum utility is increased through D2D/cellular mode selection and power allocation. The spectrum utility is defined as a combination of users' data rates, power expenditure and bandwidth. The authors first derive an optimal transmission power for the above mentioned modes, and then use evolutionary game [13] for D2D/cellular mode selection. Each user performs mode selection individually and independently. The BS collects users' mode selection decisions and broadcasts this information to all users (assisting in future mode selections). Numerical results show that, via the proposed technique, a spectrum utility can be improved when compared to solely cellular mode and D2D mode, respectively. Resource allocation method proposed in [11] is based on sequential second price auction. Here each LTE RB is put on auction, and the D2D pairs should bid for the RBs that they want to occupy. In this way, each D2D pair makes its bidding. The bidding values are represented by a function of the achievable throughput of a bidding D2D pair on the auctioned RB. Simulation results show that the achievable throughput of a proposed auction is at least 80%, a fairness index is around 0.8 and a system sum-rate efficiency is higher than 85% of the optimal resource allocation strategy.

As follows from the brief literature review provided above, D2D communication can indeed significantly improve the network performance in terms of spectrum efficiency, QoS, power reduction, etc. However, there are still some challenges that have not been addressed by previous research:

- First of all, the majority of presented techniques do not deal with the issues of D2D/cellular mode selection, spectrum assignment and interference management in a joint fashion, but rather by splitting the original problem into smaller subproblems (see, e.g., [9]), or by separating the time scales of these subproblems ([10]). Hence, although the complexity of such methods is less than the complexity of joint resource allocation, their

efficiency in terms of maximizing some certain optimality criteria is clearly downscaled.

- Secondly, most of the existing resource allocation techniques focus on improving the physical (PHY) layer network performance, measured in terms of SINR, PHY-layer throughput, power and spectrum efficiency. Such higher-layer service quality parameters, as packet delay or loss, have not been considered. Hence, the ability of these methods to improve the QoS for end-to-end user applications is questionable.
- Finally, most of the available studies are based on numerical or self-developed simulators. Such types of evaluation are suitable for studying the potential gains, but are still far from reality due to simplified assumptions. Hence, a performance evaluation using the existing network simulators, such as NS3 [14], OPNET [15], Omnet++ [16] or experimental results are necessary to reveal the actual performance of D2D communications in cellular networks.

To tackle the above challenges, an alternative resource allocation approach for D2D communication underlying LTE-A network is proposed in this paper. Here the focus is on improving the QoS of the users, measured in terms of buffer sizes of UEs. A buffer size is chosen as an optimization target because it is directly related to such higher-layer service performance metrics, as packet end-to-end delay and loss. To control the interference between cellular and D2D communication, for each user we define certain target interference levels, and constrain the interference on each wireless channel to remain below these levels. A proposed joint mode, spectrum and power allocation is implemented as part of LTE packet scheduling (the use of packet scheduling in a D2D-enabled network is described in detail in [17]), with all necessary calculations performed at the evolved NodeB (eNB). The algorithm efficiency (in terms of minimizing delay and loss for cellular and D2D users) is evaluated using simulations in OPNET environment.

The rest of the paper is organized as follows. The model of a D2D-enabled LTE-A network and a resource allocation problem are formulated in Section II. A solution methodology and the implementation of a proposed joint mode, spectrum and power allocation algorithm are described in Section III. A simulative performance analysis of the algorithm is presented in Section IV. The paper is finalized in Conclusion.

II. RESOURCE ALLOCATION PROBLEM

A. Network Model

In this paper, the problem of resource allocation for D2D communication is investigated for both the uplink (UL) and the downlink (DL) directions. Similarly, the discussion through the rest of the paper is applicable (if not stated otherwise) to either direction. Consider a basic LTE-A network which consists of one eNB operating on a fixed spectrum band spanning K RBs numbered RB_1, \dots, RB_K . Let $\mathbf{K} = \{1, \dots, K\}$ be the set of the all RBs' indices comprising

the available bandwidth. Described network operates on a slotted-time basis with the time axis partitioned into equal non-overlapping time intervals (slots) of the length T_s , with t denoting an integer-valued slot index.

The eNB serves N wireless users numbered U_1, \dots, U_N . Let $\mathbf{N} = \{1, \dots, N\}$ be the set of users' indices. Note that in LTE system, the number of users, as well as the unique users' identification numbers (IDs) can be found from the standard random access channel (RACH) procedure, which is used for initial access to the network (i.e., for originating, terminating or registration call) [18], [19]. It is assumed that each UE can operate either in a traditional cellular mode or in D2D mode (in which case it communicates on the underlay to cellular communication). In this work, the modes (D2D or cellular) of the users are selected dynamically based on results of resource allocation. Consequently, let us define a binary mode allocation variable $c_n(t)$, $n \in \mathbf{N}$, equaling 1 if U_n selects to operate in cellular mode at slot t , and 0 otherwise.

Note that in LTE system, the RBs are allocated to the users by the eNB using the packet scheduling procedure (described in detail in [19]). As part of packet scheduling, each cellular user is required to collect and transmit its instantaneous buffer status information (bit arrival rate and buffer size in bits) at every slot t . In this way, the eNB gets to "know" the exact amount of the UL data arrived and enqueued in the buffers of UEs. In the DL direction, the size of the DL buffer for each cellular user can be readily observed at the eNB at any slot t . In the framework described in this paper, both the cellular and D2D users adopt the above scheduling procedure. Let us further define a binary RB allocation variable $b_n^k(t)$, $n \in \mathbf{N}$, $k \in \mathbf{K}$, equaling 1 if U_n is allocated with RB_k at slot t , and 0 otherwise. It is assumed that each RB is allocated to at most one cellular user, whereas the number of D2D users operating on the same RBs is unlimited. Hence,

$$\sum_{n \in \mathbf{N}} c_n(t) b_n^k(t) \leq 1, \forall k \in \mathbf{K}. \quad (1)$$

Recall that both the single carrier frequency division multiple access (SC-FDMA) and orthogonal frequency division multiple access (OFDMA), applied in the UL and DL of LTE system, grant the orthogonality of resource allocation to different cellular users located within one cell (i.e., when no frequency reuse is considered) [18]. In other words, the transmissions of cellular users can be distorted only by the D2D users operating on the same RB(s), whereas the transmissions of D2D users may be affected by both the cellular and D2D users. Let G_{nm}^k denote the channel gain coefficient between the transmitter-receiver pair U_n and U_m operating on RB_k , for any $n, m \in \mathbf{N}$, $k \in \mathbf{K}$. Note, that in LTE the instantaneous values of G_{nm}^k for the UL and DL directions can be obtained from the CSI through the use of special reference signals (RSs) [20]. This information is known by the eNB and the users.

Then, at any slot t , the SINR for U_n operating on RB_k , equals [21]

$$\text{SINR}_n^k(t) = \frac{p_n(t) b_n^k(t) G_{nn}^k}{\sum_{m \in \mathbf{N} \setminus \{n\}} p_m(t) b_m^k(t) G_{nm}^k + N_0}, \forall n \in \mathbf{N}, \forall k \in \mathbf{K} \quad (2)$$

where $p_n(t)$ is the transmission power (in Watts) allocated to U_n at slot t . The denominator of (2) is a sum of the following two components: i) the additive white Gaussian noise (AWGN) power denoted N_0 and ii) the interference from the other users operating on RB_k , given by

$$I_n^k(t) = \sum_{m \in \mathbf{N} \setminus \{n\}} p_m(t) b_m^k(t) G_{nm}^k, \forall n \in \mathbf{N}, \forall k \in \mathbf{K}. \quad (3)$$

Because of the condition (1), if U_n operates in cellular mode (with $c_n(t) = 1$), then the interference in (3) will be created only by the D2D user(s) transmitting over RB_k . On the contrary, the transmissions of U_n operating in D2D mode (with $c_n(t) = 0$) can be affected by at most one cellular user and one or more D2D users operating on RB_k .

In (2) and (3), the power levels of the users should be non-negative and cannot exceed some predefined limits. Let P_n and P_{eNB} be the maximal possible transmission power levels (in Watts) of U_n and the eNB, respectively. That is,

$$0 \leq (1 - c_n(t)) p_n(t) \leq P_n, \forall n \in \mathbf{N} \quad (4a)$$

for D2D users. For the users operating in cellular mode, we have

$$0 \leq c_n(t) p_n(t) \leq P_n, \forall n \in \mathbf{N} \quad (4b)$$

for the UL direction

$$0 \leq \sum_{n \in \mathbf{N}} c_n(t) p_n(t) \leq P_{eNB} \quad (4c)$$

for the DL direction.

B. Problem Statement

In a D2D model described above, the users operating in different modes share the same RBs, which can significantly increase the spectrum efficiency of a network. Another advantage of the underlay D2D communication is the possibility of QoS provisioning for the users within the cellular (licensed) spectrum [22]. Consequently, there are two main challenges of resource allocation for a D2D-enabled cellular network:

- 1) The modes, RBs and transmit power levels of the users should be allocated effectively to maintain their traffic demands and improve their QoS.
- 2) The interference between different users operating on the same RBs should be kept at the desired level (this can be done by controlling the power of individual UEs).

To tackle the first challenge of resource allocation, it is necessary to choose an appropriate and easily obtainable system parameter to measure the users' QoS and then optimize it during resource allocation. In this regard, most of the existing techniques focus only on providing the PHY-layer service performance. However, D2D communication can also be used to improve such higher-layer QoS metrics as packet delay and loss, which is very important for real-time applications (e.g., on-line games and multimedia). In LTE system, unfortunately, the direct estimation of delay and loss is rather complex. For instance, the end-to-end packet delay in LTE consists of various components, including transmission and queuing delays, propagation and processing delays, the UL delay due to scheduling and a delay due to hybrid

automatic repeat request (HARQ) [23]. The accurate analysis of these delay components requires knowledge of many system parameters which may be not available during resource allocation.

It is worth mentioning that in many past works (e.g., [3], [5]) the total service rate of the users has been maximized during resource allocation. Although the sum rate maximization objective is very important from the point of view of the network operators, it also has some negative sides:

- First of all, the sum rate maximization does not allow to control the QoS of each end-user (unless some delay/buffer size constraints are included in formulation);
- In addition, this objective does not guarantee the fairness of resource allocation, because the user with higher demand can be allocated less capacity than a user with lower demand.

Based on above considerations, we suggest the size of UEs' buffers as a service performance measure. The main reasons behind such choice are the following. First of all, the buffer size of UE is directly related to its packet delay and loss. Secondly, at any slot t , the buffer size can be easily estimated using a well-known Lindley's equation [23]

$$q_n(t+1) = \lceil q_n(t) + a_n(t) - r_n(t) \rceil^+, \forall n \in \mathbf{N} \quad (5)$$

where $\lceil x \rceil^+ = \max(0, x)$; $q_n(t)$ is the buffer size (in bits) of U_n at slot t ; $a_n(t)$ is the bit arrival rate (in bits per slot or bps) of U_n at slot t ; $r_n(t)$ is the bit service rate (in bps) of U_n at slot t .

Note that at any slot t , the values of $q_n(t)$, $a_n(t)$ can be collected at a corresponding U_n . Parameter $r_n(t)$ depends on the number of RBs and the transmission power allocated to U_n at slot t . In LTE system, $r_n(t)$ can be calculated using the modified Shannon expression [24], as follows:

$$r_n(b_n^1(t), \dots, b_n^K(t), p_n(t)) = \omega\psi \sum_{k \in \mathbf{K}} b_n^k(t) \log(1 + g(\text{SINR}_n^k(t)) \cdot \text{SINR}_n^k(t)), \forall n \in \mathbf{N}. \quad (6)$$

In (6), ω is the bandwidth of one RB ($\omega = 180$ kHz); the parameter ψ represents the system bandwidth efficiency; the function $g(\cdot)$ determines the SINR efficiency of the transmission channel of U_n [24]. A more detailed description of ψ and $g(\cdot)$ will be provided in Section III. With buffer size as a QoS measure, at each slot t the resources can be allocated to minimize the maximal buffer size of the users at the next slot $t+1$. This will help to minimize the possibility of network congestion, as well as to decrease delay and loss for the users.

To meet the second challenge of resource allocation, it is enough to specify some target interference level I_n^{tar} for each user U_n , and constrain the inference for U_n to stay below this level¹. That is,

$$\sum_{k \in \mathbf{K}} I_n^k(t) \leq I_n^{\text{tar}}, \forall n \in \mathbf{N}. \quad (7)$$

Now, given the conditions (1), (4), (7) and the objective to minimize the maximum buffer size of the users in (5), a resource allocation problem can be readily formulated. To simplify notation, the index t is omitted below and further in

the paper. First, let us define the binary $N \times K$ -dimensional RB allocation matrix and the N -dimensional mode and power allocation vectors as

$$\mathbf{b} := \begin{bmatrix} b_1^1 & \dots & b_1^K \\ \vdots & \vdots & \vdots \\ b_N^1 & \dots & b_N^K \end{bmatrix}, \mathbf{c} := \begin{bmatrix} c_1 \\ \vdots \\ c_N \end{bmatrix}, \mathbf{p} := \begin{bmatrix} p_1 \\ \vdots \\ p_N \end{bmatrix}. \quad (8)$$

The sets of all admissible values that the optimization variables \mathbf{b} , \mathbf{c} and \mathbf{p} can take are given by

$$\mathbf{B} := \left\{ \mathbf{b} \mid \sum_{n \in \mathbf{N}} c_n b_n^k \leq 1, b_m^k \in \{0, 1\}, \forall m \in \mathbf{N}, \forall k \in \mathbf{K} \right\}; \quad (9)$$

$$\mathbf{C} := \left\{ \mathbf{c} \mid c_n \in \{0, 1\}, \forall n \in \mathbf{N} \right\}; \quad (10)$$

$$\mathbf{P} := \left\{ \mathbf{p} \mid 0 \leq p_n \leq P_n, \forall n \in \mathbf{N} \right\}, \quad (11a)$$

respectively, for the UL direction, and

$$\mathbf{P} := \left\{ \mathbf{p} \mid 0 \leq \sum_{n \in \mathbf{N}} c_n p_n \leq P_{\text{eNB}}, 0 \leq (1 - c_m) p_m \leq P_m, \forall m \in \mathbf{N} \right\} \quad (11b)$$

for the DL direction.

Given the optimization variables defined in (8), the feasibility sets (9) - (11) and the target interference constraint (7), the resource allocation problem is formulated as

$$\text{minimize } \max_{n \in \mathbf{N}} \lceil q_n + a_n - r_n(\mathbf{b}, \mathbf{p}) \rceil^+ \quad (12a)$$

$$\text{subject to: } \mathbf{b} \in \mathbf{B}, \mathbf{c} \in \mathbf{C}, \mathbf{p} \in \mathbf{P} \quad (12b)$$

$$\sum_{m \in \mathbf{N} \setminus \{n\}} p_m \sum_{k \in \mathbf{K}} b_m^k b_n^k G_{nm}^k \leq I_n^{\text{tar}}, \forall n \in \mathbf{N}. \quad (12c)$$

In above formulation the service rates of the users are expressed explicitly as the functions of \mathbf{b} and \mathbf{p} . Note that all necessary information (the sets \mathbf{N} , \mathbf{K} and the values of G_{nm}^k , q_n , a_n) is reported to the eNB for all $n, m \in \mathbf{N}$, $k \in \mathbf{K}$, using the standard control signaling defined in LTE system. Based on this information, the eNB solves (12), and then reports the optimal components of $(\mathbf{b}^*, \mathbf{c}^*, \mathbf{p}^*)$ to respective users. The advantage of such centralized approach is that the processing capabilities of the eNB are much better than those of the UEs, and therefore the eNB is able to solve the problems much faster than if it would be done by user devices. A solution methodology for (12) will be presented in the next Section.

III. ALGORITHM IMPLEMENTATION

A. Bandwidth Efficiency and SINR Efficiency

In real LTE networks, the bandwidth efficiency and the SINR efficiency are strictly less than 1 due to numerous reasons [24]. The bandwidth efficiency ψ is reduced because of the several overheads on link and system levels. Hence, it is fully determined by the design and internal settings of a system, and does not depend on PHY-layer characteristics of the wireless channels. The SINR efficiency is mainly limited by the maximum efficiency of a supported modulation and coding scheme (MCS) [24]. In LTE, MCS is chosen using adaptive modulation and coding (AMC) to maximize the data rate by adjusting transmission parameters to the current channel conditions. AMC is one of the realizations of dynamic link adaptation. In AMC algorithm, the appropriate MCS indices for packet transmissions are assigned periodically by

¹ Some possible settings of I_n^{tar} will be discussed in the next Section.

the eNB based on instantaneous channel conditions reported by the users. The period for MCS allocation is usually equal one slot. The higher MCS indices are assigned to the channels with good channel quality (to achieve higher transmission rate). The lower MCS indices are allocated to the channels with poor channel quality to decrease the transmission rate and ensure the transmission quality [25], [26].

The method for MCS selection is expressed as follows. The LTE standard allows 15 MCS indices. Note that the SINR in wireless channels varies according to instantaneous radio channel conditions and power allocations. Depending on SINR, the corresponding MCS index is chosen as [26]

$$MCS = \begin{cases} MCS_1, & SINR < \gamma_1 \\ MCS_2, & \gamma_1 \leq SINR < \gamma_2 \\ \vdots & \vdots \\ MCS_{15}, & \gamma_{14} \leq SINR < \gamma_{15} \end{cases} \quad (13a)$$

In (13a), the values $\gamma_1 < \gamma_2 < \dots < \gamma_{15}$ are the SINR thresholds for selecting the corresponding MCS index. Table I shows the MCS indices k , respective values of SINR efficiency ζ_k , and the SINR thresholds γ_k . Figure 1 shows the SINR efficiency $g(SINR)$ for different values of SINR. In (6), we have represented this explicitly as the function

$$g(SINR) = \begin{cases} \zeta_1, & SINR < \gamma_1 \\ \zeta_2, & \gamma_1 \leq SINR < \gamma_2 \\ \vdots & \vdots \\ \zeta_{15}, & \gamma_{14} \leq SINR < \gamma_{15} \end{cases} \quad (13b)$$

B. Solution Methodology

It is easy to check that the objective in (12) is a non-smooth non-convex function of \mathbf{b} , \mathbf{c} and \mathbf{p} . Hence, problem (12) can be cast as a non-smooth non-convex mixed non-linear integer programming (MINLP) problem, where some of the variables (particularly, the components of \mathbf{b} and \mathbf{c}) can take only binary values, whereas the components of vector \mathbf{p} are real-valued. It has been established in the past (see, e.g., [35]) that the MINLP problems involving binary variables (such as (12)) are Nondeterministic Polynomial-time (NP) hard, and the decision problem for a MINLP is NP complete. The NP-hardness proof of (12) is given in Appendix.

In general, all MINLP problems can be solved using either exact (deterministic) or heuristic techniques. A typical exact method for solving the MINLP problems is a well-known branch-and-bound algorithm [27]. Numerous heuristic methods proposed to speed-up the solution process, are local branching [28], large neighborhood search [29] and feasibility pump [30], to name a few. In any MINLP method, a solution process involves solving a continuous relaxation of the problem (the problem without integer restrictions) [27]. In our case, such relaxation is given by

$$\text{minimize } \max_{n \in \mathbf{N}} [q_n + a_n - r_n(\mathbf{b}, \mathbf{p})]^+ \quad (14a)$$

$$\text{subject to: } \mathbf{b} \in \tilde{\mathbf{B}}, \mathbf{c} \in \tilde{\mathbf{C}}, \mathbf{p} \in \mathbf{P} \quad (14b)$$

$$\sum_{m \in \mathbf{N} \setminus \{n\}} p_m \sum_{k \in \mathbf{K}} b_n^k b_m^k G_{mn}^k \leq I_n^{tar}, \forall n \in \mathbf{N} \quad (14c)$$

where

$$\tilde{\mathbf{B}} := \left\{ \mathbf{b} \mid \sum_{n \in \mathbf{N}} c_n b_n^k \leq 1, 0 \leq b_m^k \leq 1, \forall m \in \mathbf{N}, \forall k \in \mathbf{K} \right\}; \quad (14d)$$

$$\tilde{\mathbf{C}} := \{ \mathbf{c} \mid 0 \leq c_n \leq 1, \forall n \in \mathbf{N} \}. \quad (14e)$$

Note that (14) is equivalent to

$$\text{minimize } q^{\max} \quad (15a)$$

$$\text{subject to: } \mathbf{b} \in \tilde{\mathbf{B}}, \mathbf{c} \in \tilde{\mathbf{C}}, \mathbf{p} \in \mathbf{P} \quad (15b)$$

$$\sum_{m \in \mathbf{N} \setminus \{n\}} p_m \sum_{k \in \mathbf{K}} b_n^k b_m^k G_{mn}^k \leq I_n^{tar}, \forall n \in \mathbf{N} \quad (15c)$$

$$q_n + a_n - q^{\max} \leq r_n(\mathbf{b}, \mathbf{p}) \leq q_n + a_n, \forall n \in \mathbf{N}. \quad (15d)$$

TABLE I. MCS INDICES, ASSOCIATED MODULATION AND CODE RATE, SINR EFFICIENCIES AND THRESHOLDS IN LTE STANDARD [25]

MCS indices, MCS_k	Modulation	Code Rate	SINR Efficiency, ζ_k	SINR Thresholds (dB), γ_k
0	No transmission			
1	QPSK	78	0.1523	-3.1
2	QPSK	120	0.2344	-1.2
3	QPSK	193	0.3770	1.5
4	QPSK	308	0.6016	4
5	QPSK	449	0.8770	6
6	QPSK	602	1.1758	8.9
7	16QAM	378	1.4766	12.7
8	16QAM	490	1.9141	14.9
9	16QAM	616	2.4063	17.5
10	64QAM	466	2.7305	20.5
11	64QAM	567	3.3223	22.5
12	64QAM	666	3.9023	23.2
13	64QAM	772	4.5234	24.9
14	64QAM	873	5.1152	27

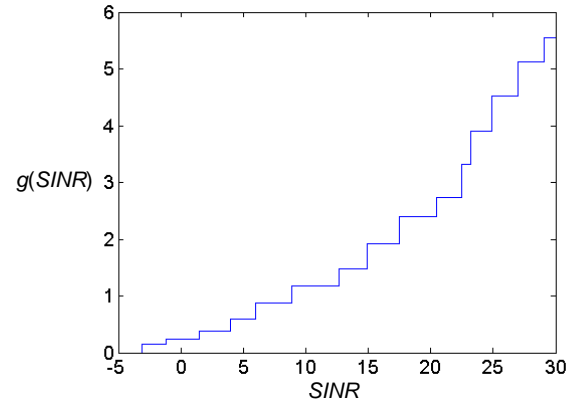


Figure 1. The SINR efficiency $g(SINR)$ for different SINR values [25].

Problem (15) is a non-smooth non-convex optimization problem. Hence, existing local convex programming methods cannot be applied to solve the problem (15) in its current form. However, we can construct a sequence of smooth approximations \hat{g}_q , $q \in \mathbf{Z}^+$, such that

$$\lim_{q \rightarrow \infty} \hat{g}_q = g$$

and solve (15) using a sequential optimization approach as follows:

$$(\mathbf{b}^*, \mathbf{c}^*, \mathbf{p}^*) = \arg \min_{(\mathbf{b}, \mathbf{c}, \mathbf{p})} q^{\max} \quad (16a)$$

$$\text{subject to: } \mathbf{b} \in \tilde{\mathbf{B}}, \mathbf{c} \in \tilde{\mathbf{C}}, \mathbf{p} \in \mathbf{P} \quad (16b)$$

$$\sum_{m \in \mathbf{N} \setminus \{n\}} p_m \sum_{k \in \mathbf{K}} b_n^k b_m^k G_{mn}^k \leq I_n^{\text{tar}}, \forall n \in \mathbf{N} \quad (16c)$$

$$\sum_{k \in \mathbf{K}} b_n^k \log(1 + \hat{g}(\text{SINR}_n^k) \cdot \text{SINR}_n^k) \leq \frac{q_n + a_n}{\omega\psi}, \forall n \in \mathbf{N} \quad (16d)$$

$$\sum_{k \in \mathbf{K}} b_n^k \log(1 + \hat{g}(\text{SINR}_n^k) \cdot \text{SINR}_n^k) \geq \frac{q_n + a_n - q^{\max}}{\omega\psi}, \forall n \in \mathbf{N}. \quad (16e)$$

It is easy to check, that $g(x)$ is equivalent to a sum of the shifted and scaled versions of the Heaviside step function $H(x)$ [31] given by

$$g(x) = \sum_{k=1}^{15} (\zeta_k - \zeta_{k-1}) H(x - \gamma_k); \quad (17a)$$

$$H(x) = \begin{cases} 1, & \text{if } x \geq 0 \\ 0, & \text{otherwise} \end{cases} \quad (17b)$$

where $\zeta_0 = 0$.

Recall that a smooth approximation for a step function $H(x)$ is given by a logistic sigmoid function [32]

$$\hat{H}_q(x) = \frac{1}{1 + e^{-2qx}}$$

where $q > 0$, x is in range of real numbers from $-\infty$ to $+\infty$. If we take $H(0) = 1/2$, then a larger q corresponds to a closer transition to $H(x)$, i.e.

$$\lim_{q \rightarrow \infty} \hat{H}_q(x) = H(x).$$

Above holds, because for $x < 0$, we have

$$e^{-2qx} \rightarrow +\infty, \hat{H}_q(x) \approx H(x) = 0;$$

for $x > 0$,

$$e^{-2qx} \rightarrow 0, \hat{H}_q(x) \approx H(x) = 1;$$

for $x = 0$,

$$e^{-2qx} = 1, \hat{H}_q(x) = H(x) = 1/2.$$

Consequently, an approximation for a shifted Heaviside function is represented by a shifted logistic function

$$\hat{H}_q(x - \gamma_k) = \frac{1}{1 + e^{-2q(x - \gamma_k)}}, \quad (18)$$

defined for $q > 0$, and real x in range from $-\infty$ to $+\infty$.

Based on (18), we can construct a smooth approximation for $g(x)$ as

$$\hat{g}_q(x) = \sum_{k=1}^{15} (\zeta_k - \zeta_{k-1}) \hat{H}_q(x - \gamma_k) = \sum_{k=1}^{15} \frac{\zeta_k - \zeta_{k-1}}{1 + e^{-2q(x - \gamma_k)}}. \quad (19)$$

Then, it is rather straightforward to verify that

$$\lim_{q \rightarrow \infty} \hat{g}_q(x) = g(x).$$

In fact, the approximation is rather close, as it follows from the example in Figure 2 showing the graphs of $g(x)$ and $\hat{g}_q(x)$ for $q = 5$ and $q = 10$.

With the approximation given by (19), the problem (16) can be solved locally using any standard non-convex optimization technique. In this paper, a second-order interior point algorithm modified for non-convex problems (as it has been done, for instance, in [33]) is applied to solve (16). This

method has been chosen mainly due to its (relatively) low complexity. Its worst-case complexity for finding an ε -scaled second order stationary point (where the Hessian matrix is positive semidefinite) is $O(\varepsilon^{-3/2})$ for a given accuracy $0 \leq \varepsilon \leq 1$ (see [34] for proof). In our case, an ε global minimizer is defined as a feasible solution $(\mathbf{b}_\varepsilon, \mathbf{c}_\varepsilon, \mathbf{p}_\varepsilon)$, such that

$$f(\mathbf{b}_\varepsilon, \mathbf{c}_\varepsilon, \mathbf{p}_\varepsilon) - \min_{\mathbf{b}, \mathbf{c}, \mathbf{p}} (q^{\max} + I_F(\mathbf{b}, \mathbf{c}, \mathbf{p})) \leq \varepsilon$$

where $f(\mathbf{b}_\varepsilon, \mathbf{c}_\varepsilon, \mathbf{p}_\varepsilon)$ is the value of the objective (16a) in a feasible point $(\mathbf{b}_\varepsilon, \mathbf{c}_\varepsilon, \mathbf{p}_\varepsilon)$; $I_F(\mathbf{b}, \mathbf{c}, \mathbf{p})$ is the indicator function of a feasibility set \mathbf{F} , given by

$$I_F(\mathbf{b}, \mathbf{c}, \mathbf{p}) = \begin{cases} 0, & \mathbf{b}, \mathbf{c}, \mathbf{p} \in \mathbf{F} \\ +\infty, & \mathbf{b}, \mathbf{c}, \mathbf{p} \notin \mathbf{F} \end{cases}$$

$$\mathbf{F} := \left\{ (\mathbf{b}, \mathbf{c}, \mathbf{p}) \left| \begin{array}{l} \sum_{m \in \mathbf{N} \setminus \{n\}} p_m \sum_{k \in \mathbf{K}} b_n^k b_m^k G_{mn}^k \leq I_n^{\text{tar}} \\ \sum_{k \in \mathbf{K}} b_n^k \log(1 + \hat{g}(\text{SINR}_n^k) \cdot \text{SINR}_n^k) \leq \frac{q_n + a_n}{\omega\psi} \\ \sum_{k \in \mathbf{K}} b_n^k \log(1 + \hat{g}(\text{SINR}_n^k) \cdot \text{SINR}_n^k) \geq \frac{q_n + a_n - q^{\max}}{\omega\psi} \\ \mathbf{b} \in \tilde{\mathbf{B}}, \mathbf{c} \in \tilde{\mathbf{C}}, \mathbf{p} \in \mathbf{P}, \forall n \in \mathbf{N} \end{array} \right. \right\}$$

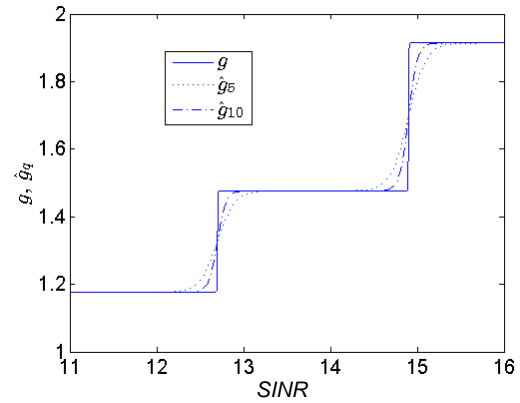


Figure 2. Original function $g(x)$ and its approximations for $q = 5$ and 10 .

If there is a feasible solution to (16), we are done (and a solution to the original problem (12) is found). Otherwise, a solution to (16) yields a lower bound for the MINLP problem, and we apply some suitable technique to find the optimal/near-optimal result. Among the various integer programming methods, there are only a few that can be used for solving non-convex problems [35]. Feasibility Pump (FP) heuristic for non-convex MINLPs ([35], [36]) is perhaps the most simple and most effective for producing more and better solutions in a shorter average running time. Its complexity is exponential in size of a problem for the problems with non-binary integer variables, and polynomial for the problems with binary variables [37]. The local convergence property of FP algorithm for non-convex problems has been proved in [36].

The fundamental idea of FP heuristic is to decompose a problem into two parts: integer feasibility and constraint feasibility. The former is achieved by rounding (solving a convex relaxation to the original problem), the latter - by projection (solving a continuous relaxation). Consequently, two sequences of points are generated: the first sequence

$\{(\overline{\mathbf{b}}, \mathbf{c}, \mathbf{p})_i\}_{i=1}^I$, $I \in \mathbf{Z}^+$ containing the integral points that may violate the non-convex constraints; the second sequence $\{(\underline{\mathbf{b}}, \mathbf{c}, \mathbf{p})_i\}_{i=1}^I$ containing the points which are feasible for a continuous relaxation to the original problem but might not be integral.

More specifically, with input $(\underline{\mathbf{b}}, \mathbf{c}, \mathbf{p})_i$ being a solution to (16), the algorithm generates two sequences by solving the following problems for $i = 1, \dots, I$:

$$(\underline{\mathbf{b}}, \mathbf{c}, \mathbf{p})_i = \arg \min \|(\mathbf{b}, \mathbf{c}, \mathbf{p}) - (\underline{\mathbf{b}}, \mathbf{c}, \mathbf{p})_i\|_1 \quad (20a)$$

$$\text{subject to: } \mathbf{b} \in \mathbf{B}, \mathbf{c} \in \mathbf{C}, \mathbf{p} \in \mathbf{P} \quad (20b)$$

$$\sum_{m \in \mathbf{N} \setminus \{n\}} p_m \sum_{k \in \mathbf{K}} b_n^k b_m^k G_{mn}^k \leq I_n^{tar}, \forall n \in \mathbf{N}; \quad (20c)$$

$$(\overline{\mathbf{b}}, \mathbf{c}, \mathbf{p})_{i+1} = \arg \min \|(\mathbf{b}, \mathbf{c}, \mathbf{p}) - (\overline{\mathbf{b}}, \mathbf{c}, \mathbf{p})_{i+1}\|_2 \quad (21a)$$

$$\text{subject to: } \mathbf{b} \in \tilde{\mathbf{B}}, \mathbf{c} \in \tilde{\mathbf{C}}, \mathbf{p} \in \mathbf{P} \quad (21b)$$

$$\sum_{m \in \mathbf{N} \setminus \{n\}} p_m \sum_{k \in \mathbf{K}} b_n^k b_m^k G_{mn}^k \leq I_n^{tar}, \forall n \in \mathbf{N} \quad (21c)$$

$$\sum_{k \in \mathbf{K}} b_n^k \log(1 + \hat{g}(SINR_n^k) \cdot SINR_n^k) \leq \frac{q_n + a_n}{\omega\psi}, \forall n \in \mathbf{N} \quad (21d)$$

$$\sum_{k \in \mathbf{K}} b_n^k \log(1 + \hat{g}(SINR_n^k) \cdot SINR_n^k) \geq \frac{q_n + a_n - q^{\max}}{\omega\psi}, \forall n \in \mathbf{N} \quad (21e)$$

where $\|\cdot\|_1$ and $\|\cdot\|_2$ are l_1 norm and l_2 norm, respectively, defined as

$$\|(\mathbf{b}, \mathbf{c}, \mathbf{p}) - (\underline{\mathbf{b}}, \mathbf{c}, \mathbf{p})_i\|_1 := \sum_{n \in \mathbf{N}} \left\{ \sum_{k \in \mathbf{K}} |b_n^k - \underline{b}_{n,i}^k| + |c_n - \underline{c}_{n,i}| + |p_n - \underline{p}_{n,i}| \right\};$$

$$\|(\mathbf{b}, \mathbf{c}, \mathbf{p}) - (\overline{\mathbf{b}}, \mathbf{c}, \mathbf{p})_i\|_2 := \sqrt{\sum_{n \in \mathbf{N}} \left\{ \sum_{k \in \mathbf{K}} |b_n^k - \overline{b}_{n,i}^k|^2 + |c_n - \overline{c}_{n,i}|^2 + |p_n - \overline{p}_{n,i}|^2 \right\}}$$

where $\underline{b}_{n,i}^k, \underline{c}_{n,i}, \underline{p}_{n,i}$ and $\overline{b}_{n,i}^k, \overline{c}_{n,i}, \overline{p}_{n,i}$ are the components of $(\underline{\mathbf{b}}, \mathbf{c}, \mathbf{p})_i$ and $(\overline{\mathbf{b}}, \mathbf{c}, \mathbf{p})_i$, respectively; $|x|$ denotes the absolute value of x .

A rounding step is carried out by solving the problem (20), whereas a projection is the solution to (21). A suggested FP algorithm alternates between the rounding and projection steps until $(\overline{\mathbf{b}}, \mathbf{c}, \mathbf{p})_i = (\underline{\mathbf{b}}, \mathbf{c}, \mathbf{p})_i$ (which implies feasibility) or the number of iterations i has reached the predefined limit I . A workflow of the corresponding FP algorithm is illustrated in Figure 3.

0. Initialization: input I ; set $i := 1$; solve (16) to obtain $(\underline{\mathbf{b}}, \mathbf{c}, \mathbf{p})_i$;

1. If $(\underline{\mathbf{b}}, \mathbf{c}, \mathbf{p})_i$ **is feasible then** goto step 7;

2. While ($i < I$) **do:**

{

3. Rounding: solve (20) to obtain $(\overline{\mathbf{b}}, \mathbf{c}, \mathbf{p})_i$;

4. If $(\overline{\mathbf{b}}, \mathbf{c}, \mathbf{p})_i = (\underline{\mathbf{b}}, \mathbf{c}, \mathbf{p})_i$ **then** goto step 7;

5. Projection: solve (21) to obtain $(\underline{\mathbf{b}}, \mathbf{c}, \mathbf{p})_{i+1}$;

6. Set $i := i + 1$;

}

7. Output: solution $(\mathbf{b}^*, \mathbf{c}^*, \mathbf{p}^*) := (\underline{\mathbf{b}}, \mathbf{c}, \mathbf{p})_i$.

Figure 3. FP algorithm for solving non-convex MINLP.

The problem (21) is very similar to (16), and therefore it can be solved using the same technique described in [33]. Problem (20) is convex MINLP which can be solved to optimality by at least five different algorithms [27]. These are branch-and-bound method [38], generalized Benders decomposition [39], outer approximation [40], branch-and-cut algorithm [41] and the extended cutting plane technique [42]. In general, any of these methods can be applied to solve (20) [27]. In this work, a modification of the branch-and-bound technique proposed in [38] has been used to solve this problem.

C. Target Interference Levels

Note that some users may operate on very noisy channels, and further reduction of SINR in these channels will be disastrous. To indicate such channels, for each user U_n operating on any RB, we set some target SINR level $SINR_n^{tar}$ (below which the data transmission is considered unsatisfactory). Then, at any slot t , we keep the SINR in all wireless channels above this target level. That is,

$$SINR_n^k = \frac{p_n b_n^k G_{nn}^k}{\sum_{m \in \mathbf{N} \setminus \{n\}} p_m b_n^k b_m^k G_{nm}^k + N_0} \geq SINR_n^{tar}, \forall n \in \mathbf{N}, \forall k \in \mathbf{K}. \quad (22)$$

Based on (22), the interfering users are allowed to transmit at the level

$$\sum_{k \in \mathbf{K}} I_n^k = \sum_{m \in \mathbf{N} \setminus \{n\}} p_m \sum_{k \in \mathbf{K}} b_n^k b_m^k G_{nm}^k \leq \frac{p_n \sum_{k \in \mathbf{K}} b_n^k G_{nn}^k}{SINR_n^{tar}} - \sum_{k \in \mathbf{K}} b_n^k N_0, \forall n \in \mathbf{N} \quad (23)$$

and the target interference I_n^{tar} can be set equal

$$I_n^{tar} = \frac{p_n \sum_{k \in \mathbf{K}} b_n^k G_{nn}^k}{SINR_n^{tar}} - \sum_{k \in \mathbf{K}} b_n^k N_0, \forall n \in \mathbf{N}. \quad (24)$$

The right-hand side of equality (24) depends on the current RB and power assignments, \mathbf{b} and \mathbf{p} , which are unknown at the moment of resource allocation (i.e., at slot t). Therefore, instead of current values of \mathbf{p} and \mathbf{b} , we deploy past (available) observations of \mathbf{p} and \mathbf{b} , and set

$$I_n^{tar} = \frac{\bar{p}_n \sum_{k \in \mathbf{K}} \bar{b}_n^k G_{nn}^k}{SINR_n^{tar}} - \sum_{k \in \mathbf{K}} \bar{b}_n^k N_0, \forall n \in \mathbf{N} \quad (25a)$$

where

$$\bar{p}_n = \frac{\sum_{\tau=1}^T p_n(t-\tau)}{T}, \bar{b}_n^k = \frac{\sum_{\tau=1}^T b_n^k(t-\tau)}{T}, \forall n \in \mathbf{N}, \forall k \in \mathbf{K}. \quad (25b)$$

In (25b), T is the number of past observations; \bar{p}_n and \bar{b}_n^k are the time averaged components of a power allocation vector and a RB allocation matrix, respectively. The value of T can be determined based on the following considerations. First of all, T should be long enough to capture the trending levels of power and RB allocation. However, because of time-varying wireless channel quality, the observation period should not exceed the fluctuation periodicity of SINR in time domain. According to a recent study [43], the minimum and mean SINR fluctuation periods (for fixed users) are equal 7 and 25 ms, respectively. Consequently, for LTE slot size $T_s = 1$ ms, we can choose any value of T , such that $7 \leq T \leq 25$.

IV. PERFORMANCE EVALUATION

A. Simulation Model

A simulation model of the network has been implemented upon a standard LTE-A platform using the OPNET simulation and development package [15]. The model consists of one eNBs serving N UEs, randomly positioned in a service area with 500 m radius. The eNB operates on a fixed spectrum band spanning $B = 50$ RBs (which is equivalent to 10 MHz). A radio model of the network has been developed according to ITU-T Recommendation M.1225. The maximal transmission power of each eNBs is assumed to be equal $P_{eNB} = 46$ dBm. The maximal transmission power of each UE is $P_n = 23$ dBm, for all $n \in \mathbf{N}$. The accuracy of a second-order interior point algorithm [33] is set to be equal $\varepsilon = 0.001$; the number of iterations in FP algorithm is limited to $I = 200$. The system parameters of a network are set in accordance with the requirements of LTE specifications [18] (the main simulation parameters are listed in Table II).

TABLE II. SIMULATION PARAMETERS OF THE MODEL

Parameter	Value	
Radio Network Model:	Path loss	$L=40\log_{10}R+30\log_{10}f+49$, where R is the distance (km), f is the carrier frequency (Hz)
	Shadow fading	Log-normal shadow fading with a standard deviation of 10/12 dB for outdoor/indoor users
	Penetration loss	The average building penetration loss is 12 dB with a standard deviation of 8 dB
	Multipath fading	Spatial channel model (SCM), suburban macro
	UE velocity	0 km/s
	Transmitter/receiver antenna gain	10 dBi (pedestrian), 2 dBi (indoor)
	Receiver antenna gain	10 dBi (pedestrian), 2 dBi (indoor)
	Receiver noise figure	5 dB
	Thermal noise density	-174 dBm/Hz
	Cable/connector/combiner losses	2 dB
PHY-Layer Profile:	Operation mode	Frequency division duplex (FDD)
	Cyclic prefix type	Normal (7 Symbols per slot)
	Evolved packet core (EPC) bearer definitions	348kbit/s, non-guaranteed bear rate (GBR)
	Subcarrier spacing	15kHz
Admission Control Parameters:	PHY DL control channel (PDCCH) symbols per subframe	3
	UL loading factor	1
	DL loading factor	1
	Inactive bearer timeout	20 sec
Buffer Status Report Parameters:	Periodic timer	5 subframes
	Retransmission timer	2560 subframes
Layer 1/Control Parameters:	Reserved size	2 RBs
	Cyclic shifts	6
	Starting resource block	0
	preserver (RBP) for Format 1 messages	
	Allocation periodicity	5 subframes
Random Access (RA)	Number of preambles	64
	Preamble format	Format 0 (1-subframe long)

Parameters:	Number of RA resources per frame	4
	Preamble retransmission limit	5 subframes
	RA Response Timer	5 subframes
	Contention Resolution Timer	40 subframes
	HARQ Parameters:	Maximal number of retransmissions
	HARQ retransmission timer	8 subframes (UL and DL)
	Maximal number of HARQ processes	8 per UE (UL and DL)

The user traffic in simulations consists of three most frequently used network applications: voice over internet protocol (VoIP), video and hypertext transfer protocol (HTTP). The number of users of each type is distributed in proportion 2:3:5 for voice, video and data users, respectively. The voice, video and data services are modelled according to [44], as follows:

- The VoIP applications are simulated using ON-OFF model with exponentially distributed ON-OFF periods. The mean duration of ON and OFF periods are 0.65s and 0.352s, respectively. The VoIP traffic is generated by using the G.723.1 (12.2 Kbps) codec with a voice payload size 40 bytes and a voice payload interval 30 ms.
- Video services are simulated using a high resolution video model with a constant frame size equal 6250 bytes and exponentially distributed frame inter-arrival intervals (with mean equal 0.5s).
- Web users in simulations are HTTP1.1 users generating pages or images with exponential page inter-arrival intervals (mean equal 60sec). It is assumed that one page consists of one object, whereas one image consists of five objects. The object size is constant and equal 1000 bytes.

The target SINR levels for UEs are determined according to their QoS requirements, and are set equal 5, 10 and 15 dB for web, video and VoIP users, respectively. The target interference level I_n^{tar} for each U_n is calculated using (25), based on a specified $SINR_n^{tar}$, with $T = 10$ slots.

In this work, the performance of a proposed resource allocation algorithm (denoted as a queue-based control or QBC) is compared with the performance of two most relevant schemes proposed previously:

- The first scheme, a graph-based resource allocation (GRA), has already been introduced in Section I. In GRA, the RBs are assigned to different cellular and D2D users based on interference-awareness (defined as a condition that the BS can acquire local awareness on the channel gains) of each wireless link. The basic idea of GRA is to iteratively gather vertices from the clusters of cellular/D2D users into the corresponding clusters of the same RB, taking both the interference and the channel capacity values into account to guarantee that the service rate of each cluster is maximized. This iterative RB assignment process cycles until all the cellular/D2D clusters are empty. A

more detailed description of GRA can be found in [3].

- In a second scheme, proposed in [9] (also listed in Section I), the mode, channel and transmission power are assigned to UEs to minimize their total power consumption. It is based on the following two procedures: i) mode selection that uses a linear search to determine transmission modes (D2D or cellular) of the users based on their power consumption and ii) channel/power assignment to determine the sub-channels and transmission power allocated to each D2D link based on the outcome of mode selection. A second procedure is implemented in polynomial time by solving the corresponding linear programming (LP) problem (using the LP Gurobi optimizer [45]). In the following, this scheme is denoted as a joint resource allocation (JRA).

Other schemes considered in this performance evaluation study are the rate based control (RBC) and a sum queue minimization (SQM). Both of these schemes use the network model and assumptions of QBC, but have different optimization objectives. In particular, the objective of RBC is to maximize the total service rate of the users. The network resources (mode, bandwidth and power) are allocated by solving the following optimization problem:

$$\text{maximize } \sum_{n \in \mathbf{N}} r_n(\mathbf{b}, \mathbf{p}) \quad (26a)$$

$$\text{subject to: } \mathbf{b} \in \mathbf{B}, \mathbf{c} \in \mathbf{C}, \mathbf{p} \in \mathbf{P} \quad (26b)$$

$$\sum_{m \in \mathbf{N} \setminus \{n\}} p_m \sum_{k \in \mathbf{K}} b_n^k b_m^k G_{mn}^k \leq I_n^{tar}, \forall n \in \mathbf{N}. \quad (26c)$$

The objective of SQM is to minimize the sum buffer size of UEs. To allocate the network resources, the algorithm solves the following problem:

$$\text{minimize } \sum_{n \in \mathbf{N}} [q_n + a_n - r_n(\mathbf{b}, \mathbf{p})]^+ \quad (27a)$$

$$\text{subject to: } \mathbf{b} \in \mathbf{B}, \mathbf{c} \in \mathbf{C}, \mathbf{p} \in \mathbf{P} \quad (27b)$$

$$\sum_{m \in \mathbf{N} \setminus \{n\}} p_m \sum_{k \in \mathbf{K}} b_n^k b_m^k G_{mn}^k \leq I_n^{tar}, \forall n \in \mathbf{N}. \quad (27c)$$

Note, that (27) is equivalent to

$$\text{maximize } \sum_{n \in \mathbf{N}} r_n(\mathbf{b}, \mathbf{p}) \quad (28a)$$

$$\text{subject to: } \mathbf{b} \in \mathbf{B}, \mathbf{c} \in \mathbf{C}, \mathbf{p} \in \mathbf{P} \quad (28b)$$

$$\sum_{m \in \mathbf{N} \setminus \{n\}} p_m \sum_{k \in \mathbf{K}} b_n^k b_m^k G_{mn}^k \leq I_n^{tar}, \forall n \in \mathbf{N}. \quad (28c)$$

$$q_n + a_n - q^{\max} \leq r_n(\mathbf{b}, \mathbf{p}) \leq q_n + a_n. \quad (28d)$$

From (28), the difference between RBC and SQM is rather straightforward. In RBC, the network resources are allocated to the users based on potential interference they may create on the allocated RBs. In SQM, not only the potential interference, but also the individual traffic demands and buffer sizes of UEs are taken into account. Note that the objective used in RBC is very important from the point of view of service providers (it maximizes the total network revenue and utilization), but may result in a rather unfair resource allocation. A methodology for solving (27) and (28) is the same as that used for solving (12). All of the schemes in this comparative performance evaluation are simulated with identical internal and external settings.

B. Simulation Results

First, we observe the complexity of different algorithms in simulations. Figures 4 and 5 demonstrate the average number of iterations necessary for convergence and the average solution time, respectively, with N varying from 10 to 150 users. In GRA, the number of iterations and the solution time shown in Figures 4 and 5, correspond to the number of RB assignment cycles necessary to empty all of the clusters. In JRA, the number of iterations and the solution time are determined from the LP algorithm used as part of the channel/power assignment procedure. Results show that QBC, RBC and SQM have a relatively low complexity (less than 70 iterations with a solution time below 100 μs for the network with $N = 150$ users). These results verify that the deployed FP heuristic is rather effective in producing fast solutions. The complexities of JRA and GRA are also not very high (in both algorithms, the reported worst-time complexity is polynomial).

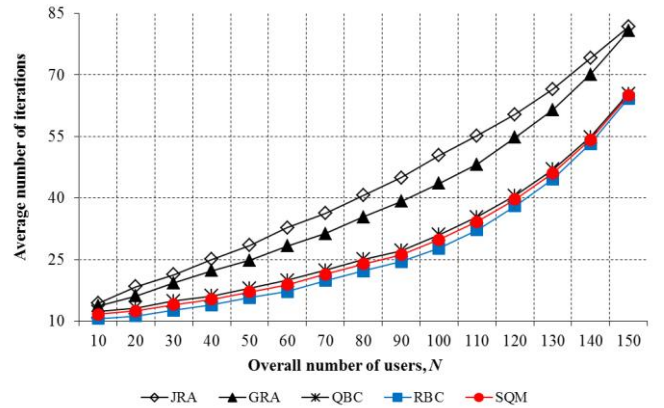


Figure 4. Average number of iterations in different algorithms for N varying from 10 to 150 users.

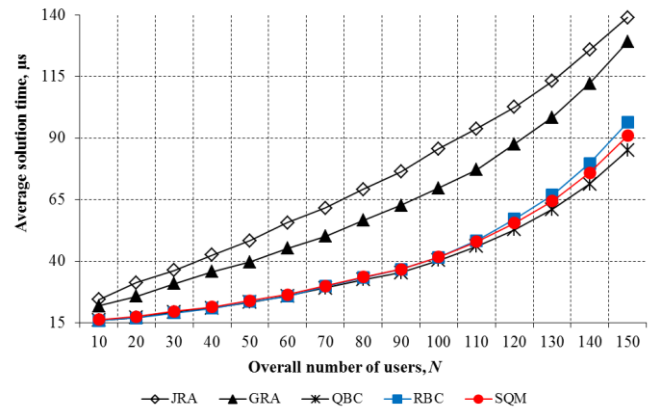


Figure 5. Average solution time in different algorithms for N varying from 10 to 150 users.

Next, we observe the performance of different schemes in terms of mean packet end-to-end delay, loss and SINR for the users operating in cellular and D2D modes. The graphs in Figures 6 - 10 present simulation results for N varying from 10 to 150 users. It follows from these graphs that the mean packet delay and loss for D2D users are less than those for cellular

users in all schemes, which is simply explained by the fact that the D2D users communicate with each other, and the delay and loss associated with transmissions between the eNB and corresponding UEs are nulled.

Results also show that JRA has the worst performance in terms of mean packet end-to-end delay and loss in the network. This is because this scheme was originally designed to facilitate green communication (by minimizing the total transmission power of the users), and therefore the achieved delay/loss performance for UEs is not satisfactory. All the other algorithms either maximize the total network throughput (GRA and RBC) or minimize the total/maximum buffer size (SQM and QBC). Hence, their delay/loss outcome is more satisfactory. The minimal delay and loss are attained by QBC and SQM (with a slightly better performance of QBC) since both of these schemes take into account the buffer status information. In terms of mean SINR, all algorithms show rather similar performance (Figure 10). This is explained by the actions that all of the schemes take towards the interference protection for the users operating in cellular or D2D mode (although the means of protection used by different schemes are disparate).

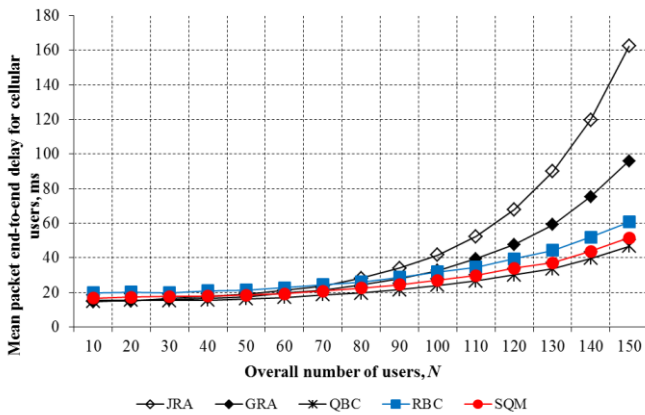


Figure 6. Mean packet end-to-end delay for the users operating in cellular mode with N varying from 10 to 150 users.

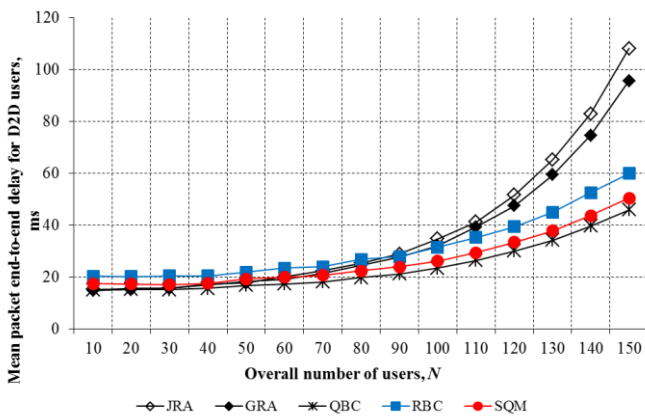


Figure 7. Mean packet end-to-end delay for the users operating in D2D mode with N varying from 10 to 150 users.

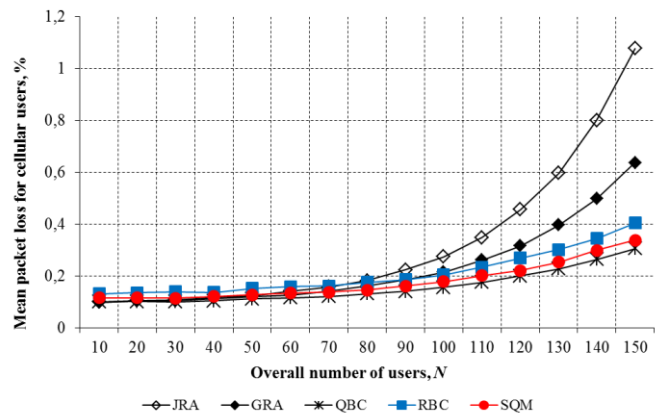


Figure 8. Mean packet loss for the users operating in cellular mode with N varying from 10 to 150 users.

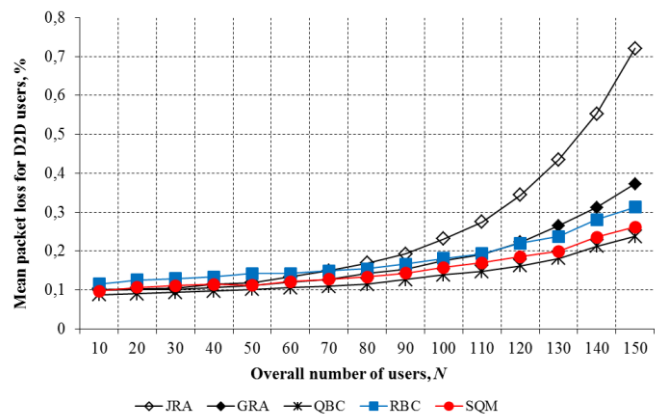


Figure 9. Mean packet loss for the users operating in D2D mode with N varying from 10 to 150 users.

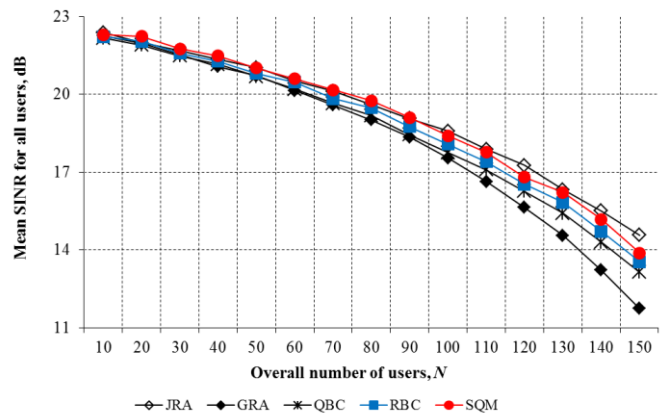


Figure 10. Mean SINR for the users operating in either mode with N varying from 10 to 150 users.

CONCLUSION

In this paper, the D2D/cellular mode selection, resource allocation and interference management scheme for a D2D-enabled LTE-A network has been presented. The aim of the proposed algorithm is to improve the user-perceived QoS (counted in terms of buffer size of UEs). To control the interference between cellular and D2D communication, the interference for each user is constrained to stay below a

certain target interference level. The algorithm efficiency has been evaluated using the OPNET-based simulations. The algorithm has shown improved performance in terms of mean packet end-to-end delay and loss for both the D2D and cellular users when compared to other relevant schemes.

APPENDIX

To prove that (12) is NP-hard, we first show that the problem

$$\text{minimize } \max_{n \in \mathbf{N}} [q_n + a_n - r_n(\mathbf{b}, \mathbf{p})]^+ \quad (\text{A.1a})$$

$$\text{subject to: } g_k(\mathbf{b}, \mathbf{c}) = \sum_{n \in \mathbf{N}} c_n b_n^k - 1 \leq 0, \forall k \in \mathbf{K} \quad (\text{A.1b})$$

$$g_{K+n}(\mathbf{b}, \mathbf{c}, \mathbf{p}) = \sum_{m \in \mathbf{N} \setminus \{n\}} p_m \sum_{k \in \mathbf{K}} b_n^k b_m^k G_{mm}^k - I_n^{\text{tar}} \leq 0, \forall n \in \mathbf{N} \quad (\text{A.1c})$$

$$b_n^k \in \{0, 1\}, c_n \in \{0, 1\}, p_n \in \{0, 1\}, \forall n \in \mathbf{N}, \forall k \in \mathbf{K}. \quad (\text{A.1d})$$

is NP-hard.

Lemma 1. Problem (A.1) is NP-hard.

Proof: In order to prove that (A.1) is NP-hard, it is enough to show that its corresponding decision problem² is NP-complete [46]. Note, that the decision version of (A.1) is NP-complete if

- 1) (A.1) is in NP, and
- 2) there is an NP-complete problem Π , such that Π is polynomial time reducible³ to (A.1).

The fact that (A.1) is contained in NP is easy to verify. Suppose that the instance of (A.1) has a feasible solution $(\mathbf{b}^*, \mathbf{c}^*, \mathbf{p}^*)$ with

$$\max_{n \in \mathbf{N}} [q_n + a_n - r_n(\mathbf{b}, \mathbf{p})]^+ \leq \chi.$$

The binary encoding size of $(\mathbf{b}^*, \mathbf{c}^*, \mathbf{p}^*)$ is $N \times (K+2)$ (since \mathbf{b}^* is a binary matrix with $N \times K$ entries, \mathbf{c}^* and \mathbf{p}^* are the binary vectors with N entries each). Hence, we can check in polynomial time that $(\mathbf{b}^*, \mathbf{c}^*, \mathbf{p}^*)$ is a feasible solution by checking all the constraints and the objective function value. This gives us a certificate that the instance of (A.1) is a “yes”-instance (i.e., a decision problem of asking whether a given input $(\mathbf{b}^*, \mathbf{c}^*, \mathbf{p}^*)$ is feasible, holds an answer “yes”), and therefore (A.1) is in NP.

We now show that some other NP-complete problem Π can be “formulated” as (A.1) with a polynomial reduction. In particular, we reduce the satisfiability (SAT) problem [47] to (A.1). Note that the NP-completeness of SAT has been proved in Cook’s Theorem [47]. Suppose we are given an instance of SAT with the input being a set of $N+K$ clauses⁴ $\{C_1, \dots, C_{N+K}\}$ involving $N(K+2)$ Boolean variables $x_1, \dots, x_{N(K+2)}$. Each clause contains conjunction (\wedge), disjunction (\vee) and

negation (\neg) operators. Given the SAT formula $\varphi = C_1 \wedge C_2 \wedge \dots \wedge C_{N+K}$, the question posed is whether there exists an assignment of truth values to the variables, such that all clauses are satisfiable.

In the following, we construct a problem based on a SAT instance. For each Boolean variable x_i , let there be a corresponding optimization variable in (A.1), such that

$$b_n^k \Leftrightarrow x_{N(k-1)+n}, c_n \Leftrightarrow x_{NK+n}, p_n \Leftrightarrow x_{N(K+1)+n}, \forall n \in \mathbf{N}, \forall k \in \mathbf{K}.$$

The possible values of x_i are true and false; these will be encoded as 1 and 0, respectively, for each component of $(\mathbf{b}, \mathbf{c}, \mathbf{p})$. We denote by C_j^+ and C_j^- , $j = 1, \dots, NK$, the index sets of positive and negative literals in a clause C_j , respectively. For each clause C_j , $j = 1, \dots, N+K$, let g_j be a constraint contained in either (A.1b) or (A.1c). Note that the Boolean conjunction and disjunction in SAT instance correspond to the multiplication and addition, respectively, in arithmetic expressions. Consequently, the clauses C_1, \dots, C_K corresponding to the constraints g_1, \dots, g_K in (A.1b) are given by

$$C_k = \bigvee_{n \in \mathbf{N}} x_{NK+n} \wedge x_{N(k-1)+n}, \forall k \in \mathbf{K}.$$

The clauses C_{K+1}, \dots, C_{K+N} corresponding to the constraints g_{K+1}, \dots, g_{K+N} in (A.1c) are described by

$$C_{K+n} = \bigvee_{m \in \mathbf{N} \setminus \{n\}} \{x_{N(K+1)+m} \wedge (\bigvee_{k \in \mathbf{K}} x_{N(k-1)+n} \wedge x_{N(k-1)+m})\}, \forall n \in \mathbf{N}.$$

Now, we add the following constraint to the instance of (A.1):

$$\sum_{i \in C_j^+} x_i + \sum_{i \in C_j^-} (1 - x_i) \geq 1, \quad j = 1, \dots, N+K. \quad (\text{A.2})$$

It is easy to check that (A.1) can be set up in polynomial time given the instance of SAT. First, we prove that a “yes”-instance of SAT yields a “yes”-instance of (A.1). Let $x_1^*, \dots, x_{N(K+2)}^*$ be a truth assignment that evaluates to true in the SAT formula φ . In a clause C_j , these must be at least one true variable in C_j^+ or at least one false variable in C_j^- . Setting $x_i^* = 1$ for each true variable and $x_i^* = 0$ for each false variable will satisfy the constraint (A.2). Thus, a feasible SAT instance yields a feasible instance of (A.1), which completes the proof.

We next prove that a “yes”-instance of (A.1) brings in a “yes”-instance of SAT. Let $(\mathbf{b}^*, \mathbf{c}^*, \mathbf{p}^*)$ be a feasible instance of (A.1). In a constraint g_j , at least one variable in C_j^+ must be equal to 1, or at least one variable in C_j^- must be equal to 0 to satisfy (A.2). Setting each literal x_i to true in the SAT formula φ if the corresponding variable equals 1 in $(\mathbf{b}^*, \mathbf{c}^*, \mathbf{p}^*)$, and setting x_i to false otherwise, we ensure that each clause evaluates to true since at least one literal in C_j^+ will be true or at least one literal in C_j^- will be false, which completes the proof.

Now, since each feasible instance of SAT yields a feasible instance of (A.1), and vice versa, it follows that (A.1) has a feasible solution if and only if the given instance of SAT is satisfiable. \square

Lemma 2. Problem (12) is NP-hard.

Proof: Lemma 2 can be proved similar to Lemma 1. To show that (12) is NP-hard, we have to verify that

- 1) (12) is in NP, and

² A decision problem is a question which can be answered “yes” or “no”, depending on the values of some input, which is called an instance of the problem [46].

³ In complexity theory, a polynomial time reduction of a problem Π to a problem Π' is a polynomial time computable function f with the property that $x \in \Pi$ if and only if $f(x) \in \Pi'$. We say that Π is polynomial time reducible to Π' if there exists a polynomial time reduction from Π to Π' . If we have a way of reducing instances of Π into instances of Π' , then solving Π' is theoretically at least as difficult as solving Π [46].

⁴ In Boolean algebra, a clause is a logical expression which contains one or more literals. A literal is either a variable (then called positive literal) or the negation of a variable (then called negative literal) [46].

2) there is an NP-complete problem Π , such that Π is polynomial time reducible to (12).

The fact that (12) is contained in NP can be proved as follows. Suppose that the instance of (12) has a feasible solution $(\mathbf{b}^*, \mathbf{c}^*, \mathbf{p}^*)$ with

$$\max_{n \in \mathbf{N}} [q_n + a_n - r_n(\mathbf{b}, \mathbf{p})]^+ \leq \chi.$$

Note, that the components p_n of the N -dimensional vector \mathbf{p}^* are the rational numbers, and therefore they can be represented as

$$p_n = \frac{\alpha_n}{\beta_n}, \quad \alpha_n \in \mathbf{Z}, \beta_n \in \mathbf{N}$$

where \mathbf{Z} and \mathbf{N} are the set of integers and natural numbers, respectively; α_n and β_n do not have a common divisor other than 1. Hence, the encoding length of p_n equals [46]

$$\langle p_n \rangle := 1 + \lceil \log_2(|\alpha_n| + 1) \rceil + \lceil \log_2(\beta_n + 1) \rceil \quad (\text{A.3})$$

where $\langle x \rangle$ denotes the binary encoding size of x ; $\lceil x \rceil$ and $|x|$ are the ceiling and the absolute value of x , respectively. Then, the binary encoding length of a rational N -dimensional vector \mathbf{p} is given by

$$\langle \mathbf{p} \rangle := N + \sum_{n \in \mathbf{N}} \langle p_n \rangle. \quad (\text{A.4})$$

Based on (A.4), the encoding size of $(\mathbf{b}^*, \mathbf{c}^*, \mathbf{p}^*)$ is

$$\langle \mathbf{b}^* \rangle + \langle \mathbf{c}^* \rangle + \langle \mathbf{p}^* \rangle := N \times (K + 2) + \sum_{n \in \mathbf{N}} \langle p_n^* \rangle$$

(since \mathbf{b}^* is a binary matrix with $N \times K$ entries, \mathbf{c}^* is a binary vector which consist of N components). Consequently, we can check in polynomial time that $(\mathbf{b}^*, \mathbf{c}^*, \mathbf{p}^*)$ is a feasible solution (by checking all the constraints and the objective function value), which gives us a certificate that the instance of (12) is a “yes”-instance. Hence, (12) is contained in NP.

To prove that there exists an NP-complete problem Π , which is polynomial time reducible to (12), note that (12) is a generalization of an NP-complete problem (A.1). Therefore, (A.1) can be reduced to (12) in polynomial time. \square

REFERENCES

- [1] C.-H. Yu et. al., On the performance of device-to-device underlay communication with simple power control, in Proc. IEEE VTC, 2009, pp. 1-5.
- [2] K. Doppler et. al., Device-to-device communication as an underlay to LTE-advanced networks, IEEE Commun. Mag., vol. 47, no. 12, pp. 42-49, 2009.
- [3] R. Zhang et. al., Interference-aware graph based resource sharing for device-to-device communications underlying cellular networks, in Proc. IEEE WCNC, 2013, pp. 140-145.
- [4] X. Chen et. al., Downlink resource allocation for device-to-device communication underlying cellular networks, in Proceedings of IEEE PIMRC, 2012, pp. 232-237.
- [5] C. Xu et. al., Resource allocation using a reverse iterative combinatorial auction for device-to-device underlay cellular networks, in Proc. IEEE GLOBECOM, 2012, pp. 4542-4547.
- [6] D. Feng et. al., Device-to-device communications underlying cellular networks, IEEE Transactions on Communications, vol. 61, no. 8, pp. 3541-3551, 2013.
- [7] L. Su et. al., Resource allocation using particle swarm optimization for D2D communication underlay of cellular networks, in Proc. IEEE WCNC, 2013, pp. 129-133.
- [8] M.-H. Han, B.-G. Kim, and J.-W. Lee, Subchannel and transmission mode scheduling for D2D communication in OFDMA networks, in Proc. IEEE VTC-Fall, 2012, pp. 1-5.
- [9] G. Chenfei et.al., Joint mode selection, channel allocation and power assignment for green device-to-device communications, in Proc. ICC, 2014, pp. 178-183.
- [10] P. Cheng et. al., Resource allocation for cognitive networks with D2D communication: An evolutionary approach, in Proc. IEEE WCNC, 2012, pp. 2671-2676.
- [11] C. Xu et. al., Interference aware resource allocation for device-to-device communications as an underlay using sequential second price auction, in Proc. IEEE ICC, 2012, pp. 445-449.
- [12] J. Kennedy, Particle swarm optimization, in Encyclopedia of Machine Learning. Springer, 2010, pp. 760-766.
- [13] J. W. Weibull, Evolutionary game theory. MIT press, 1997.
- [14] NS3. [Online]. Available: <http://www.nsnam.org/>
- [15] OPNET. [Online]. Available: <http://www.opnet.com/>
- [16] A. Varga, “Omnet++ simulator,” [Online]. Available: <http://www.omnetpp.org>
- [17] L. Lei et.al., Operator controlled device-to-device communications in LTE-advanced networks, IEEE Wireless Commun., vol. 19, no. 3, pp. 96 - 104, 2012.
- [18] LTE for UMTS: Evolution to LTE-Advanced. By: H. Holma and A. Toskala, John Wiley and Sons, 2011.
- [19] E-UTRA; MAC protocol specification . 3GPP TS 36.321. (Release 8).
- [20] I. F. Akyildiz, D. M. Gutierrez-Estevéz and E. C. Reyes, The evolution to 4G cellular systems: LTE-Advanced, Physical Communication, 3, 2010, pp. 217-244.
- [21] F. Baccelli and B. Błaszczyszyn, Stochastic Geometry and Wireless Networks, Volume II - Applications, 4 (1-2) of Foundations and Trends in Networking, NoW Publishers, 2009.
- [22] A. Asadi et. al., A Survey on Device-to-Device Communication in Cellular Networks, accepted for publication in IEEE Communications Surveys and Tutorials IEEE Communications Surveys and Tutorials in April 2014.
- [23] D. V. Lindley. The theory of queues with a single server. Math. Proc. of the Cambridge Philosophical Society, 48 (2): 277-289, 1952.
- [24] P. Mogensen et. al., LTE Capacity Compared to the Shannon Bound, In Proc. IEEE VTC, 2007, pp. 1234 - 1238.
- [25] Physical Channels and Modulation. 3GPP TS 36.211. (Release 8).
- [26] Multiplexing and Channel Coding. 3GPP TS 36.212. (Release 8).
- [27] S. Burer, A. N. Letchford, Non-convex mixed-integer nonlinear programming: A survey, Surveys in Operations Research and Management Science, 17, 2012, pp. 97-106.
- [28] M. Fischetti, A. Lodi, Local branching, Math. Program., 98, 2003, pp. 23-47.
- [29] A. Lodi, The heuristic (dark) side of MIP solvers. Hybrid Metaheuristics, 434, 2013, pp. 273-284.
- [30] M. De Santis, S. Lucidi, and F. Rinaldi, Feasibility pump-like heuristics for mixed integer problems, Discrete Applied Mathematics, 165, 2014, pp. 152-167.
- [31] R. Bracewell, Heaviside's Unit Step Function, $H(x)$. The Fourier Transform and Its Applications, 3rd ed. New York: McGraw-Hill, 2000, pp. 61-65.
- [32] Verhulst, Pierre-François, Notice sur la loi que la population poursuit dans son accroissement, Correspondance mathématique et physique, Vol. 10, pp. 113-121, Retrieved 2009.
- [33] R. J. Vanderbei and D. F. Shanno, An interior-point algorithm for nonconvex nonlinear programming, Computational Optimization and Applications, Vol. 13 (1-3), 1999, pp.231-252.
- [34] W. Bian, X. Chen, Y. Ye, Complexity analysis of interior point algorithms for non-Lipschitz and nonconvex minimization, Math. Program., 149 (1), 2015, pp. 301 - 327.
- [35] T. Berthold, Heuristic algorithms in global MINLP solvers, Verlag Dr. Hut, 2014.
- [36] C. D'Ambrosio et. al., A storm of feasibility pumps for nonconvex MINLP, Math. Program., 136, 2012, pp. 2012.

- [37] M. Fischetti, D. Salvagnin, Feasibility Pump 2.0, *Math. Program.*, vol. 1, no. 2-3, 2009, pp. 201-222.
- [38] S. Leyffer, Integrating SQP and branch-and-bound for mixed integer nonlinear programming, *Computational Optimization and Applications*, 18, 2001, pp. 295 - 309.
- [39] A. M. Geoffrion, Generalized benders decomposition, *J. Opt. Th. & App.*, 10, 1972, pp. 237-260.
- [40] R. Fletcher and S. Leyffer, Solving Mixed Integer Nonlinear Programs by Outer Approximation, *Math. Program.*, 66, 1994, pp. 327 - 349.
- [41] R.A. Stubbs and S. Mehrotra, A branch-and-cut method for 0-1 mixed convex programming, *Math. Program.*, 86, 1999, pp. 515 - 532.
- [42] T.Westerlund and F. Pettersson, A cutting plane method for solving convex MINLP problems, *Comput. & Chem. Eng.*, 19, 1995, pp. 131 - 136.
- [43] C. Lameiro et.al., Experimental Evaluation of Interference Alignment for Broadband WLAN Systems, arXiv preprint arXiv:1309.4355, 2015.
- [44] IPOGUE, Internet study 2007 and 2008/2009, research report.
- [45] GUROBI. [Online]. Available: <http://www.gurobi.com/>
- [46] Introduction to the theory of complexity. By: D.V. Bovet and P. Crescenzi, Prentice Hall International, 1994.
- [47] S. Cook, The complexity of theorem proving procedures, in *Proc. ACM Symposium on Theory of Computing*, 1971, pp. 151–158.